

Preliminary indirect measurement of cosmic-ray proton spectrum using Earth's γ -ray data from *Fermi* Large Area Telescope

Patomporn Payoungkhamdee

Department of Physics, Faculty of Science, Mahidol University, Bangkok 10400, Thailand

E-mail: patomporn.pay@gmail.com

Abstract. Cosmic rays (CRs) are high-energy particles, mostly protons, propagating in space. The rigidity (momentum per charge) spectrum of CRs is well described by a power law for which the spectral index is approximately 2.8 around 30 - 1000 GV. Recent measurements by PAMELA and AMS-02 indicate an abrupt change of the CR proton spectral index at about 340 GV. When CRs interact with the Earth's upper atmosphere, γ rays can be produced and detected by space-based detectors. Here we use the Earth's γ -ray data collected by the *Fermi* Large Area Telescope along with a proton-air interaction model to indirectly determine the CR proton spectral index and compare against observations by other instruments.

1. Introduction

Cosmic rays (CRs) are high energy particles mainly from outer space which can sometimes penetrate the geomagnetic field and interact with the Earth's atmosphere [1–3]. The interactions between CRs and the air molecules produce secondary particles, including γ rays, mostly in the forward direction with respect to the CR velocity. When observed from space, these CR-induced γ -ray emission of the Earth's atmosphere appears as a bright ring along the Earth's limb due to CRs grazing tangentially through the Earth's thin upper atmosphere and scattering photons towards the detector. The lower atmosphere and the physical Earth create the dark region in the center of the emission ring because they are opaque for γ rays (see figure 1 in [4]).

There are many possible acceleration mechanisms in space that could produce high energy particles. The combined effects of the acceleration, propagation, and escaping from the Galaxy result in the power-law rigidity (momentum per charge) spectrum of CRs in the form $F \propto R^\Gamma$, where F is Flux, R is rigidity, and Γ is the spectral index. Note that for relativistic energy, the rigidity value in the unit of GV is very close to being directly proportional to the kinetic energy in GeV. The CR spectral index is approximately 2.7 for a very wide rigidity range, though there are a few known changes in the index value as shown in figure 1. One is an abrupt softening at 10^{15-16} GeV, known as the “knee,” [5, 6] and the other one is a hardening at 10^{18-19} GeV, known as the “ankle” [7]. CRs produced by different sources or acceleration mechanisms may be characterized by having different spectral indices. Therefore, a spectral breaking feature could indicate a transition from a certain dominant source population of CRs to another. For example, CRs with energy above the ankle are presumably extragalactic. Finding spectral features will provide more clues to the origins of CRs.

In 2011, PAMELA indicated a sudden hardening of CR proton spectrum around 240 GV [8]. Recently in 2015, AMS-02 reported the precision measurement of the CR proton spectrum which confirmed the drastic change of the spectral index at around 336 GV [9]. As an independent cross check, in 2014 *Fermi* Large Area Telescope (LAT) used about 5 years of the CR-induced Earth's γ -ray data to indirectly observe this newly discovered spectral feature. Although the best-fit broken power-law model of CRs is consistent with the results from PAMELA and (later) AMS-02, the null hypothesis (single power-law) is rejected at only around 1σ [10]. In this work, we improve the previous LAT analysis by using a larger data set (~ 9 years) and the latest version of event selection to indirectly measure the CR proton spectral indices in the rigidity range between 60 - 2000 GV.

2. Methodology

2.1. Data selection and γ -ray flux extraction

We use ~ 9 years (7 Aug 2008 - 16 Oct 2017) of the latest version (P8R2 ULTRACLEANVETO V6) of the LAT's photon data between 10 GeV to 1 TeV. We observe γ rays from the Earth's thin upper atmosphere by selecting the nadir angle (θ_{NADIR}) from 68.4° to 70.0° [10] as demonstrated in figure 2. The incidence angle cut, $\theta_{\text{LAT}} < 70^\circ$, is also applied.

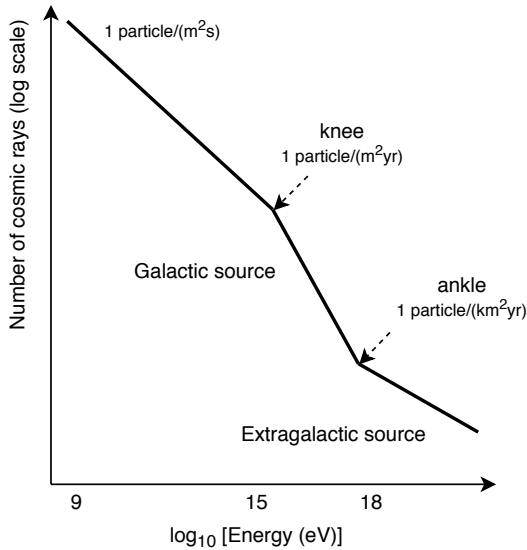


Figure 1. All-particle CR spectrum.

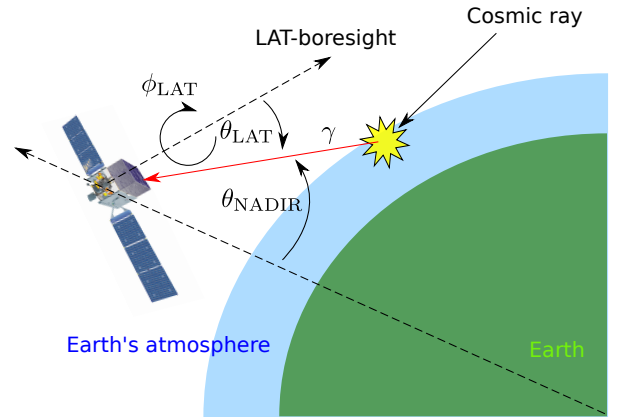


Figure 2. Schematic of high-energy Earth's γ -ray production.

The observed flux for a given energy bin is calculated using

$$\mathbf{Flux} \equiv \frac{dN_\gamma}{dE} = \frac{\int_{\text{Limb region}} (\text{Count map}/\text{Exposure map})}{\Delta\Omega\Delta E}. \quad (1)$$

Here the count map is filled with numbers of photons, the exposure map represents the exposure time as well as the effective area of spacecraft which is a function of energy and θ_{LAT} , ΔE is the energy bin width, and $\Delta\Omega$ is the solid angle of the thin-target Earth's limb region. We perform the analysis with 25 bins of energy, equally spaced in logarithmic scale. For a given energy bin, the exposure map is calculated using the spacecraft's position and orientation recorded in 30-second time steps, each of which involves a complex coordinate transformation to create a map in the zenith-azimuth system. Such computationally intensive task requires parallel processing with Master-Slave technique that we have developed.

2.2. Interaction model

In this work, we test 2 models of CR protons: single-power law (SPL) model containing one spectral index, and broken-power law (BPL) model containing two spectral indices with a break energy.

Earth's limb photons above 500 MeV are mainly from the hadronic interactions of proton-air collisions, producing neutral pions which quickly decay into pairs of γ -ray photons. According to [11], the secondary photon spectrum could be summarized by

$$\frac{dN_\gamma}{dE_\gamma} \propto \int_{E_\gamma}^{E_{\max}} dE' \frac{dN_p}{dE'} \frac{d\sigma^{pp \rightarrow \gamma}(E', E_\gamma)}{dE_\gamma}, \quad (2)$$

where here dN_γ/dE_γ is the measured Earth's limb γ -ray spectrum, dN_p/dE' is the CR proton model, and $\sigma^{pp \rightarrow \gamma}$ is the interaction cross section. We take into account the contribution from CR He particles to the production of secondary photons by using the cross section ratio ($\sigma_{\text{HeN}}/\sigma_{\text{pN}}$) from [12] and the He spectrum measurement by [13]. This modifies equation (2) to

$$\frac{dN_\gamma}{dE_\gamma}(E_\gamma) \propto \sum_{E'_i} \left[\frac{E'_i}{E_\gamma} \Delta(\ln E'_i) \right] \left[f_{pp} \frac{dN_p}{dE'_i} \left\{ 1 + \frac{\sigma_{\text{HeN}}}{\sigma_{\text{pN}}} \left(\frac{dN_p}{dR} \right)^{-1} \frac{dN_{\text{He}}}{dR} \frac{dR_{\text{He}}}{dR_p} \right\} \right], \quad (3)$$

where $f_{pp} \equiv E_\gamma(d\sigma^{ij \rightarrow \gamma}/dE_\gamma)$ is the interaction cross section table in [11].

2.3. Optimization

We use the SPL and BPL models for dN_p/dE' in equation (3) and vary their parameters (normalization, spectral indices, break energy) so that the resulting dN_γ/dE_γ from the model fits to the measured Earth's limb γ -ray spectrum with maximum likelihood. We employ the particle swarm optimization (PSO) [14] as our fitting algorithm because PSO is efficient at avoiding local maxima and reaching the global maximum in this multi-parameter problem. For the setting, we spawn 50 states of particles in hyper parameter space in which the states are randomly initialized with the spectral indices between 2.5 and 3.0, as well as the minimum and maximum breaking energy of BPL between 310 and 350 GeV. The optimization iteration process stops when the standard deviation of the log-likelihood of each particle is less than 0.1 since the particles would locate at around the same position in the parameter space when the optimization reaches the global minimum and yields similar profits.

3. Preliminary results

The optimized parameters for the SPL and BPL models are summarized in table 1. The best-fit γ -ray spectra from the two models compared to the thin-target Earth's limb measurement by the LAT are illustrated in figure 3, showing very similar results for both models. Since the proton-to- γ energy conversion factor is roughly 0.17 for broad and smooth spectra [10], our inferred CR proton spectra are valid between 60 - 2000 GV in rigidity because the lower bound is the mean rigidity of the incoming protons that produce 10-GeV γ rays. Our results are shown in comparison with measurements by other instruments in figure 4. Note that the normalizations of our work in figure 4 are scaled by fitting to AMS-02 data between 100 - 2000 GV.

4. Discussion and Future work

The best-fit BPL model of CR proton from this work are consistent with direct measurements as shown in figure 4. We will need to determine whether the BPL model fits the data significantly better than the SPL model does using likelihood ratio test to quantify the level of confidence. We also plan to determine the statistical and total uncertainties of the fit results by performing

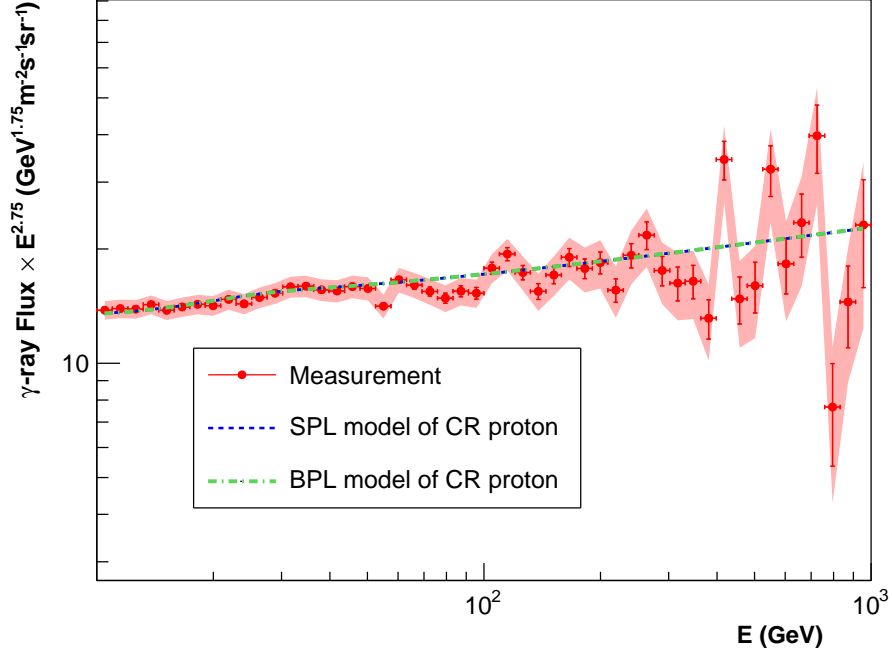


Figure 3. The γ -ray spectra calculated from the SPL (blue) and BPL (green) models of CR proton which best fit with the measured Earth's γ -ray spectrum in the thin-target regime (red).

Table 1. Best-fit CR proton spectral parameters.

CR proton model	Index 1	Index 2	E_{break} (GeV)
SPL	2.70	-	-
BPL	2.86	2.63	333

Monte Carlo simulations. This work emphasizes that we could utilize the bright γ -ray emission of the Earth's upper atmosphere to indirectly observe various properties of CRs.

Acknowledgments

I would like to express my deep gratitude to Assist. Prof. Warit Mitthumsiri and Prof. David Ruffolo for their patient guidance. I would also like to thank people at the space physics laboratory at Mahidol University for their support. This research project is partially supported by Thailand Science Research and Innovation (RTA6280002).

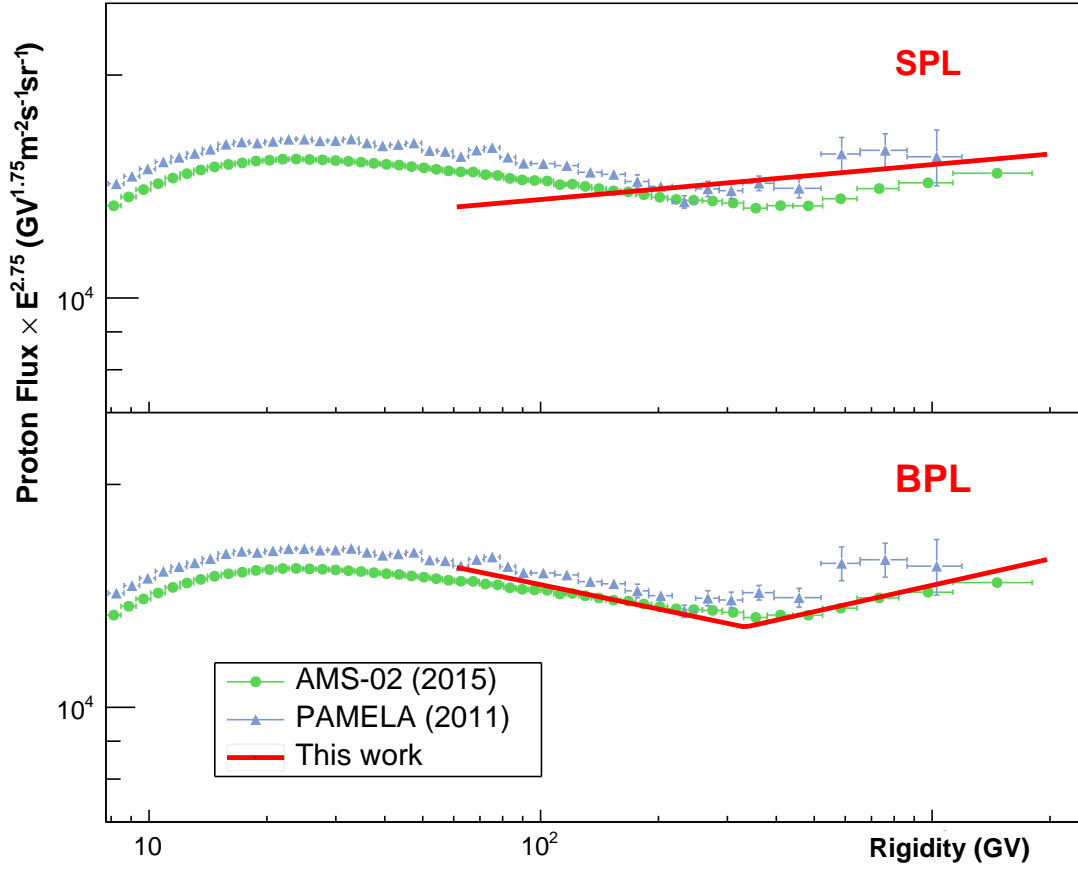


Figure 4. Best-fit CR proton spectrum from this work (red) compared to the measurements by AMS-02 (blue) and PAMELA (green).

References

- [1] Hess V F 1912 *Phys. Z.* **13** 1084
- [2] Pacini D 1912 *Il Nuovo Cimento* **3** 93
- [3] Clay J 1927 *Pro. of the Section of Sciences, Koninklijke Akademie van Wetenschappen te Amsterdam* vol 30 (Netherlands) p 1115
- [4] Abdo A A *et al.* 2009 *Phys. Rev. D* **80** 122004
- [5] Allan H R 1962 *Proc. of the Physical Society* **79** 1170
- [6] Haungs A 2003 *Rep. Prog. Phys.* **66** 1145
- [7] Abbasi R 2005 *Phys. Lett. B* **619** 271–80
- [8] Adriani O 2013 *Astrophys. J.* **765** 91
- [9] Aguilar M *et al.* 2015 *Phys. Rev. Lett.* **114** 171103
- [10] Ackermann M *et al.* 2014 *Phys. Rev. Lett.* **112** 151103
- [11] Kachelrieß M and Ostapchenko S 2012 *Phys. Rev. D* **86** 043004
- [12] Atwater T W 1986 *Phys. Rev. Lett.* **56** 1350
- [13] Aguilar M *et al.* 2015 *Phys. Rev. Lett.* **115** 211101
- [14] Kennedy J and Eberhart R 1995 *Proc. of ICNN'95 - Int. Conf. on Neural Networks* vol 4 p 1942